Int. J. Heat Mass Transfer. Vol. 13, pp. 1705–1713. Pergamon Press 1970. Printed in Great Britain

HEAT TRANSFER OF CONDENSABLE VAPOUR DIFFUSING THROUGH POROUS MEDIA

MASAO KITO

Dept. of Chem. Engineering, Gunma University, Kiryu, Japan

and

SACHIO SUGIYAMA

Dept. of Chem. Engineering, Nagoya University, Nagoya, Japan

(*Received* 23 *June* 1969)

Abstract—The transfer effect in porous media caused by condensation was treated theoretically.

The theoretical equations based on the concept of the overall specific heat were derived. The overall specific heat is defined as follows: $C_p = c_{ps} + c_{pr}$, where c_{ps} is the specific heat of the body, and c_{pr} is the value of specific heat due to the latent heat contribution.

c_{pr} is expressed by the equation $c_{pr} = \Delta H\,(\rho_v/\rho_s)\,(\partial k/\partial T)$.

The effective thermal conductivity is defined as follows: $\lambda_e = \lambda_s + \lambda_f$, where $\lambda_f = c_{pg}\rho_g pD$.

The extent of condensation within porous bodies and temperature distribution were subjected to numerical analysis by electronic computers. The theoretical data were compared with observed data.

The results of the analysis are shown in Figs. 3–6. They agree with observed results to a fair degree.

NOMENCLATURE

A, cross-sectional area [m^2];
a, distance [m];
a_v, specific surface area [m^2/m^3];
b, constant;
C_p, overall specific heat defined in equation (7) [kcal/kg °C];
c_p, specific heat [kcal/kg °C];
D, diffusion coefficient [m^2/h];
ΔH, latent heat [kcal/kg];
h, heat-transfer coefficient [kcal/m^2 h°C];
J, flux of vapour [m^3/m^2 h];
k, conversion;
kg, mass-transfer coefficient [m/h];
M, molecular weight [kg/kg mol];
P, reduced partial pressure ($= p/760$ mm Hg];
P_s, reduced saturated pressure ($= p_s/760$);
Q, heat content [kcal/m^3];
q, heat flux [kcal/m^2];
R, gas constant;
r, rate of phase transformation [kg/m^2 h];
T, temperature [°C];
t, time [h];
u, $(P - P_0)/(P_{B^\circ} - P_0)$;
V, volume of mol [m^3/mol];
x, distance [m];
y, x/a;
α, $c_{ps}\rho_s D/\lambda_s$;
β^*, ah^*/λ_s;
β^{**}, ah^{**}/λ_s;
γ^*, akg^*/D;
γ^{**}, akg^{**}/D;
ε, porosity;
ρ, density [kg/m^3];
λ, thermal conductivity [kcal/m h°C];
λ_f, thermal conductivity defined by equation (11) [kcal/m h°C];
ϑ, $(T - T_0)/(T_{B^\circ} - T_0)$;
τ, $\lambda_s t/c_p\rho_s a^2$;
ϕ, c_{pr}/c_{ps};
ψ, λ_f/λ_s.

Subscripts

B°, source value;
e, effectiveness;
g, vapour;
0, initial value;
r, latent heat contribution;
s, solid or sensible heat contribution;
*, inside;
**, outside.

INTRODUCTION

THERE are many problems concerning to the effects of condensation or vaporization affecting heat and mass transfer.

Materials for industrial use, such as lagging materials, are often covered by condensable gases, and their own properties such as thermal conductivity are changed at any rate.

Heat and mass transfer in condensation is a little different from that in drying, and methods of analyses in drying are not always applicable to estimate these effects.

This work is undertaken to define the effects of heat and mass transfer affecting the apparent thermal properties. Especially the unsteady heat transfer in some kinds of porous bodies accompanied by condensation is investigated.

BASIC EQUATIONS

A volume element of a porous body was considered as shown in Fig. 1. q_s and q_f are the heat flux attributed to conduction and diffusion, respectively. Q_r is the heat content attributed to latent heat and Q_s the heat content of solid attributed to conduction.

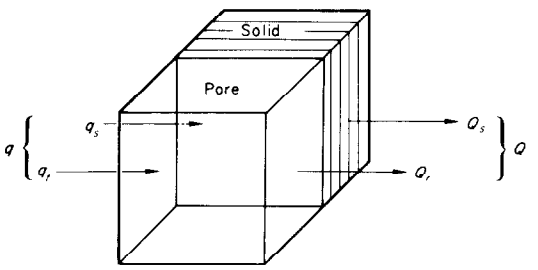

FIG. 1. Heat capacity of the volume element.

Basic equations were derived from the following assumptions:

(1) The porous body cannot be sealed by condensed vapour.
(2) Heat and mass are transported in unidirection.

$$\frac{\partial(C_p\rho T)}{\partial t} = \frac{\partial}{\partial x}\left(\lambda_e \frac{\partial T}{\partial x}\right) \tag{1}$$

$$\frac{\partial P}{\partial t} = D\frac{\partial^2 P}{\partial x^2} - P_{B^\circ}\frac{\partial k}{\partial t} \tag{2}$$

where C_p, λ_e and $(\partial k/\partial t)$ are the overall specific heat, the effective thermal conductivity and the rate of condensation respectively, which will be defined in detail later.

Initial and boundary conditions are given as follows:

initial condition $t = 0$

$$T = \text{const.}, \qquad P = \text{const.}, \qquad k = 0 \tag{3}$$

boundary condition $t > 0$

$$\left.\begin{aligned} x = a\ \lambda_e\frac{\partial T}{\partial x} &= h^*(T^* - T) \\ D\frac{\partial P}{\partial x} &= kg^*(P^* - P) \\ x = 0\ \lambda_e\frac{\partial T}{\partial x} &= h^{**}(T - T^{**}) \\ D\frac{\partial P}{\partial x} &= kg^{**}(P - P^{**}). \end{aligned}\right\} \tag{4}$$

CALCULATION METHOD

In analysing the effects caused by condensation or evaporation on the thermal properties in a system, it is assumed that the equilibrium values consist of the heat of conduction and latent heat contribution which are linearly additive.

Definition of the overall specific heat and the effective thermal conductivity

Overall specific heat. A small variation of the total heat content in any volume element is

$$dQ = dQ_s + dQ_r. \tag{5}$$

The overall specific heat C_p is defined as follows:

$$dQ = c_{ps}\rho_s\,dT \tag{6}$$

$$dQ_s = c_{ps}\rho_s\,dT_s = C_p\rho_s\,dT = (c_{ps} + c_{pr})\,\rho_s\,dT \tag{7}$$

$$C_p = c_{ps} + c_{pr} \tag{8}$$

where c_{ps} and T_s are the specific heat and the temperature of the body, respectively, and c_{pr} is the value of specific heat due to the latent heat contribution.

From equations (6) and (7), the next equation is derived;

$$c_{pr} = \frac{1}{\rho_s}\frac{dQ_r}{dT} \tag{9}$$

and by putting $dQ_r = \rho_r \Delta H\,dk$ into equation (9), we obtain

$$c_{pr} = \frac{\rho_r}{\rho_s}\Delta H\frac{\partial k}{\partial T}. \tag{10}$$

Effective thermal conductivity. The heat flux q_f caused by mass transfer is defined as follows:

$$q_f = c_{pg}\rho_g pD\frac{\partial T}{\partial x} = \lambda_f\frac{\partial T}{\partial x} \tag{11}$$

where $\lambda_f = c_{pg}\rho_g pD$.

The heat flux due to conduction q_s is equal to $\lambda_s(\partial T/\partial x)$. The total heat flux is, therefore,

$$q = q_s + q_f = \lambda_s\frac{\partial T}{\partial x} + \lambda_f\frac{\partial T}{\partial x} = \lambda_e\frac{\partial T}{\partial x} \tag{12}$$

where

$$\lambda_e = \lambda_s + \lambda_f. \tag{13}$$

Definition of the condensation rate

The condensation rate or evaporation rate may be compared with the rates of heat and mass transfer. If the former has the same magnitude as the latter, the relation between the vapour phase and the solid surface will be in non-equilibrium. The rate equation fit for such systems was proposed in the previous paper [1, 2]. In the present paper, a rate equation will be proposed for the system which is predominated by the rates of heat and mass transfer.

$$r = \rho_g\left(\frac{P}{P_s} - 1\right)J \tag{14}$$

$$\rho_g = \frac{M}{V}\frac{273}{T}P$$

$$\ln P_s = b - \frac{\Delta H}{RT}.$$

Now a conversion k will be defined as follows:

$$k = \int_0^t\int_0^{a_v} r\,da_v\,dt \Big/ \int_0^t\int_0^{\varepsilon A}\frac{P_{B^\circ}J_1}{RT_{B^\circ}}M\,dA\,dt. \tag{15}$$

From equation (15), $\partial k/\partial t$ in equation (2) will be derived as follows:

$$\frac{\partial k}{\partial t} = \frac{\partial}{\partial t}\left[\int_0^t\int_0^{a_v} r\,da_v\,dt \Big/ \int_0^t\int_0^{\varepsilon A}\frac{P_{B^\circ}J_1 r}{RT_{B^\circ}}M\,dA\,dt\right]. \tag{16}$$

And then $\partial k/\partial T$ in equation (10) is derived as follows:

$$\frac{\partial k}{\partial T} = \frac{\partial}{\partial T}\left[\int_0^t\int_0^{a_v} r\,da_v\,dt \Big/ \int_0^t\int_0^{\varepsilon A}\frac{P_{B^\circ}J_1}{RT_{B^\circ}}M\,dA\,dt\right]. \tag{17}$$

Numerical analyses

Dimensionless terms are defined as follows:

$$\vartheta = (T - T_0)/(T_{B^\circ} - T_0),$$
$$u = (P - P_0)/(P_{B^\circ} - P_0),$$
$$\tau = \lambda_s t/c_{ps}\rho_s a^2,$$
$$y = x/a,$$
$$\phi = c_{pr}/c_{ps},$$
$$\psi = \lambda_f/\lambda_s,$$
$$\alpha = c_{ps}\rho_s D/\lambda_s,$$
$$\beta^* = ah^*/\lambda_s,$$
$$\beta^{**} = ah^{**}/\lambda_s,$$
$$\gamma^* = akg^*/D,$$
$$\gamma^{**} = akg^{**}/D.$$

In the dimensionless expression, equations (1) and (2) take the following forms:

$$\frac{\partial(1+\phi)\,\vartheta}{\partial\tau} = \frac{\partial}{\partial y}\left\{(1+\psi)\frac{\partial\vartheta}{\partial y}\right\} \tag{18}$$

$$\frac{\partial u}{\partial\tau} = \alpha\frac{\partial^2 u}{\partial y^2} - \frac{\partial k}{\partial\tau}. \tag{19}$$

Similarly, initial and boundary conditions are as follows:

initial condition $\tau = 0$

$$\vartheta = 0, \qquad u = 0, \qquad k = 0 \tag{20}$$

boundary condition $\tau > 0$

$$\left.\begin{aligned} y = 1 \qquad (1+\psi)\frac{\partial\vartheta}{\partial y} &= \beta^*(\vartheta^* - \vartheta) \\ \frac{\partial u}{\partial y} &= \gamma^*(u^* - u) \\ y = 0 \qquad (1+\psi)\frac{\partial\vartheta}{\partial y} &= \beta^{**}(\vartheta - \vartheta^{**}) \\ \frac{\partial u}{\partial y} &= \gamma^{**}(u - u^{**}) \end{aligned}\right\} \tag{21}$$

In order to solve equations (18) and (21), the numerical process must be adopted.

Divide y into m equal parts and mark ϑ, u, k, ϕ and ψ with suffix i.

Equations (18) and (19) may be expressed by the differential-difference equations, as follows:

$$\frac{\mathrm{d}(1+\phi_i)\,\vartheta_i}{\mathrm{d}\tau} = \frac{1}{S^2}\{(1+\psi_{i+1,1})(\vartheta_{i+1} - \vartheta_i) - (1+\psi_{i,i-1})(\vartheta_i - \vartheta_{i-1})\} \tag{22}$$

$$\frac{\mathrm{d}u}{\mathrm{d}\tau} = \frac{\alpha}{S^2}\{(u_{i+1} - u_i) - (u_i - u_{i-1})\} - \frac{\mathrm{d}k_i}{\mathrm{d}\tau} \tag{23}$$

where if the suffix i is equal to 1 or m, equations (22) and (23) must be considered as the boundary conditions in equation (21). Next equations are consequently derived from equations (22) and (23).

$$\frac{\mathrm{d}(1+\phi_1)\,\vartheta_1}{\mathrm{d}\tau} = \frac{1}{S^2}\left\{(\psi_{21} - \psi_{10})(\vartheta_2 - \vartheta_1) - \frac{2S\beta^{**}}{1 + S\beta^*/2(1+\psi_{10})}(\vartheta_1 - \vartheta^{**})\right\}$$

$$\frac{\mathrm{d}u_1}{\mathrm{d}\tau} = \frac{\alpha}{S^2}\left\{(u_2 - u_1) + \frac{S\gamma^{**}}{1 + S\gamma^{**}/2}(u_1 - u^{**})\right\} - \frac{\mathrm{d}k_1}{\mathrm{d}\tau}$$

$$\frac{\mathrm{d}(1+\phi_m)\,\vartheta_m}{\mathrm{d}\tau} = \frac{1}{S^2}\left[S\beta^*\left\{\left(1 + \frac{W\psi_1}{1+W\psi_1}\right)\vartheta^* - \frac{1}{1+W\psi_1}\vartheta_m\right\} - (1+\psi_{m,m-1})(\vartheta_m - \vartheta_{m-1})\right]$$

$$\frac{\mathrm{d}u}{\mathrm{d}\tau} = \frac{\alpha}{S^2}\{S\gamma^*(u^* - u_m) - (u_m - u_{m-1})\} - \frac{\mathrm{d}k_m}{\mathrm{d}\tau}$$

where

$$w\psi_1 = s\beta^*/2(1+\psi_m)$$

$$\psi_{i+1,i} = (\psi_{i+1} + \psi_i)/2. \tag{24}$$

In the present numerical calculation, T_0 and P_0 are given as a standard value: T_0 is equal to room temperature and P_0 is equilibrium pressure under the condition.

Heat- and mass-transfer coefficients are evaluated from the empirical equations.

$$Nu = 0{\cdot}54\,(Gr\,.\,Pr)^{\frac{1}{4}}$$

$$Sh = 0{\cdot}55\,(Gr\,.\,Sc)^{\frac{1}{4}}.$$

Data of calculation is shown in Table 1. A digital computer HITAC 5020E for the public use at the University of Tokyo was used.

EXPERIMENTAL EQUIPMENT AND PROCEDURE

Equipment. The experimental apparatus is illustrated in Figs. 2a and 2b. The evaporator is constructed so large in scale that the vapour pressure in it should remain constant. In order to intercept the entrainments, vapour conduit pipes are arranged as shown in Fig. 2a, and a wire mesh is attached under the sample. The vapour pressure gauge is controlled by the rate of heating and control-valve opening.

A plate heat-source is shown in Fig. 2b. The temperature of it is controlled by the slide-transformer.

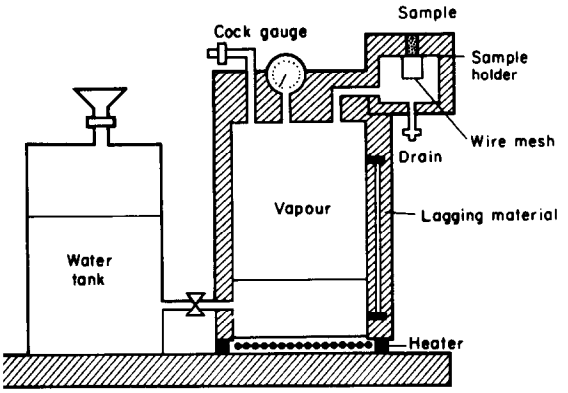

FIG. 2a. Experimental equipment.

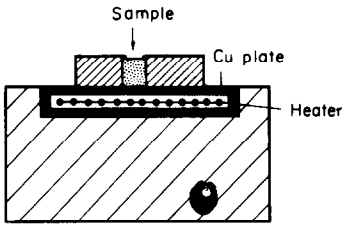

FIG. 2b. Experimental equipment.

Procedure. Samples prepared are insulating bricks (JIS grade C–1, B–1) and especially provided porous bodies. The diameter and height of samples were 3 cm and 5 cm, respectively. The side wall of them is attached to the lagging material in order to minimize heat loss from there.

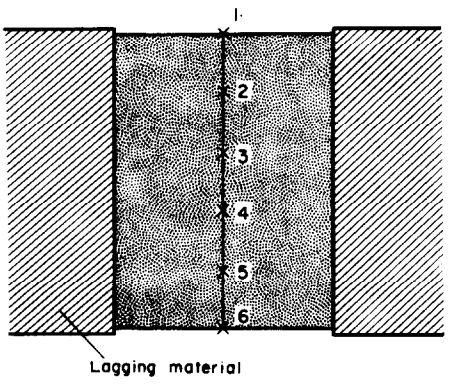

FIG. 2c. Sample.

Steam and ethanol vapour are used as condensable vapour. Noncondensable gases in liquid removed before producing vapour.

Samples are drastically dried up before testing. The moisture volume content is about 15 per cent at the end of the experimental procedures.

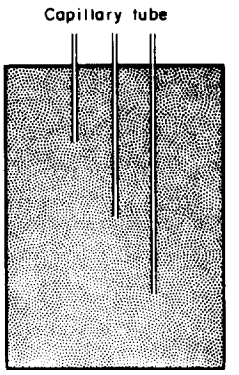

FIG. 2d. Sample.

Vapour pressure distribution in samples is measured by using capillary tubes and transducers.

Physical properties of samples are as listed in Table 1.

Table 1

λ	0·17	0·2	0·25	0·2
D	0·11	0·11	0·11	0·11
ε	0·6	0·69	0·64	0·46
ρ	$0{\cdot}7 \times 10^3$	$0{\cdot}96 \times 10^3$	$1{\cdot}18 \times 10^3$	$1{\cdot}25 \times 10^3$

Specific surface areas are calculated by equation $a_v = 6(1 - \varepsilon)/D_p$.

EXPERIMENTAL RESULTS AND DISCUSSION

The experimental and theoretical results are shown in Figs. 3–6.

Numbers (1, 2, ...) in Figs 3–6 indicate the points of temperature and pressure measurements.

In these figures, solid lines and one dot chain lines are the results due to condensation, and dotted lines and two dot chain lines are the results of cases of no condensation.

Experimental results

(a) *Cases in no condensation.* In the system shown in Figs. 3–6, the temperature distribution curves along the height of the samples are

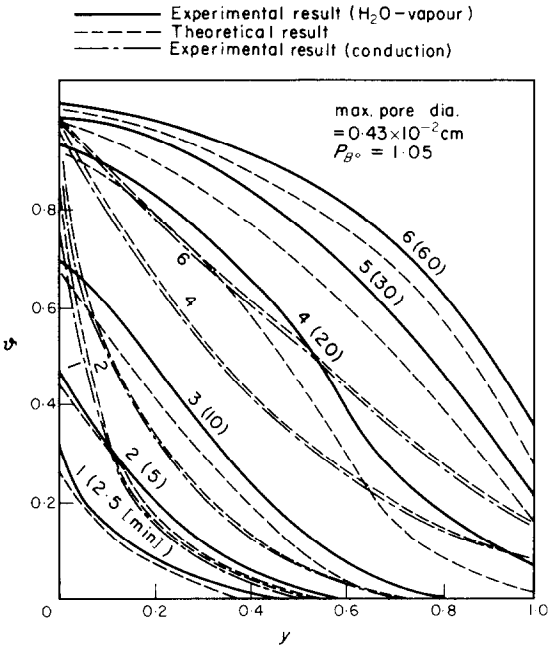

FIG. 3a. Time–temperature variation of samples.

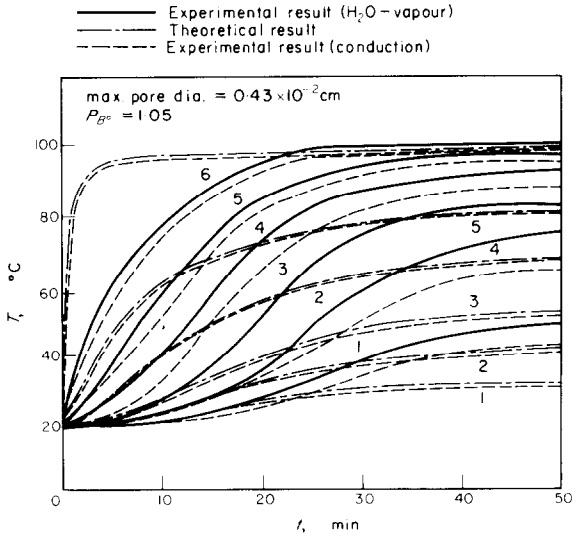

FIG. 3b. Time–temperature distribution.

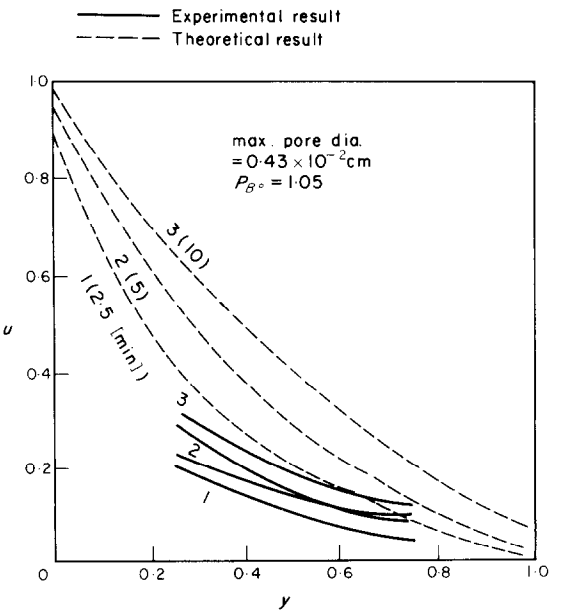

FIG. 3c. Time–pressure variation of samples.

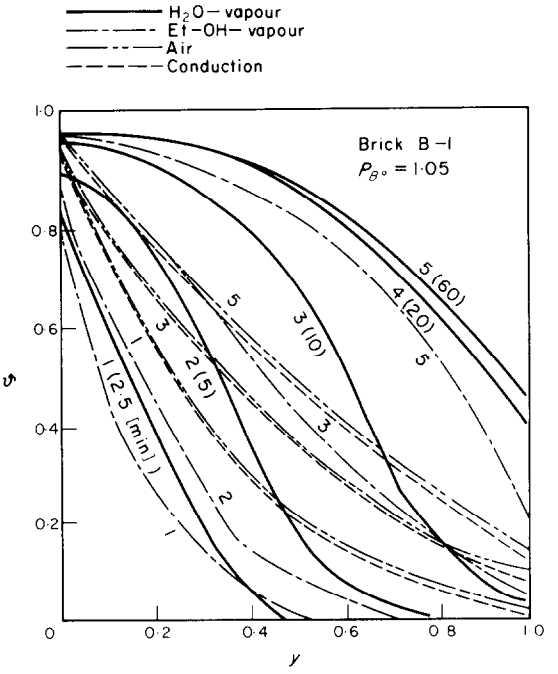

FIG. 4. Comparison of time–temperature variation of samples.

similar in each condition heated by conduction heat transfer.

In the first heating period, the temperature distribution curves have a large curvature. With the lapse of time, they shall become straight lines.

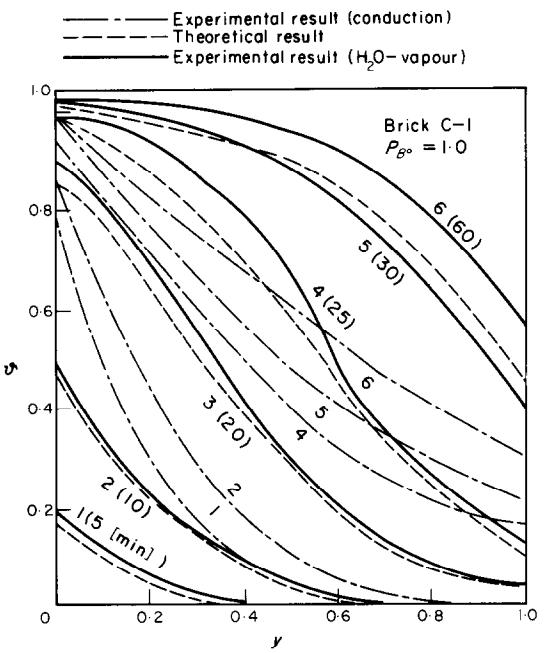

FIG. 5. Time–temperature variation of samples.

When heated air is diffused into the samples, the temperature distribution curves are the same as those of the samples heated by conductive heat transfer.

(b) *Cases in condensation.* On the other hand, when condensable vapour is diffused into the samples, the temperature distribution curves become remarkably different from the former. As shown in Figs. 3–6 (solid lines and chain lines), the curves were inversed sigmoidal in the middle period of heating and showed a small temperature gradient in the part near the vapour entrance section.

The temperature of the top of the samples is higher than that of only conductive heat transfer.

Calculated results

(a) *Cases in no condensation.* Coefficients included in equations (1)–(4) are given as follows:

$$C_p = c_{ps}, \lambda_e = \lambda_s, P = 0$$

(heating by conductive heat transfer)
and

$$C_p = c_{ps}, \Delta H = 0$$

(heating by heated air diffusion).

As shown in Figs. 3a and 3b, calculated results are in good agreement with experimental ones.

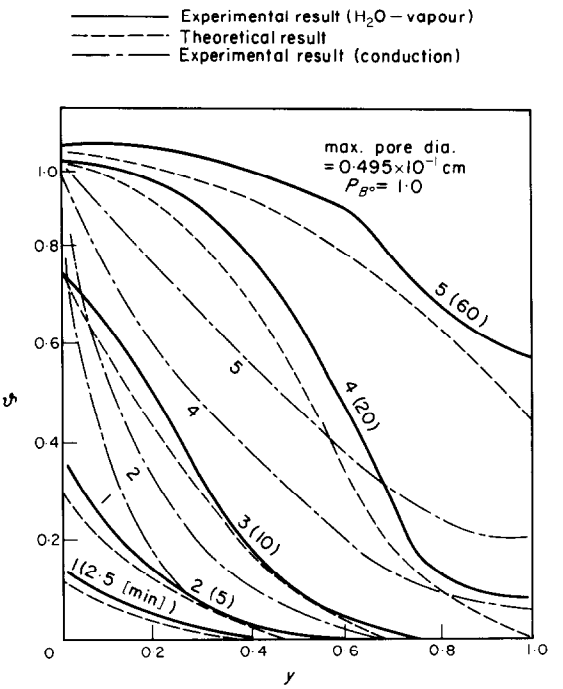

FIG. 6. Time–temperature variation of samples.

(b) *Cases in condensation.* C_p, λ_e and $\partial k/\partial t$ were given by taking latent heat into account, as indicated in equations (10), (13) and (16). When the simultaneous transport equations are integrated, the temperature profiles show a peculiar curvature and the values of temperature and pressure are comparable with the experimental ones as shown in Figs. 3–6 (broken lines).

Comparing the theoretical temperature near $x = 0$ with the experimental one, the former is lower than the latter. This may be attributed to the heat by conduction transfer from the holder fixed samples and to the calculation procedure of the specific surface area [calculated by equation $a_v = 6(1 - \varepsilon)/D_p$].

Vapour pressure distributions could not always be measured correctly because of condensation in capillary tubes.

CONCLUSION

By taking into account the simultaneous transport effects, the theoretical equations based on the concept of the overall specific heat are derived and solved numerically by using the digital computer. The overall specific heat and the effective thermal conductivity are defined by equations (8) and (13), respectively.

The calculated results of temperature and pressure profiles are compared with the observed ones.

As shown in Figs. 3–6, the calculated results are in fairly good agreement with the observed ones.

REFERENCES

1. M. KITO and S. SUGIYAMA, Effects of heat and mass transfer on the thermal decomposition of sodium bicarbonate, *Kagaku Kogaku (Chem. Engng. Japan)* **24**, 904–909 (1966).
2. M. KITO, T. ONODERA and S. SUGIYAMA, Transport phenomena accompanied by extensive variations of porosity in the solid phase, *Int. Chem. Engng* **9**, 181–188 (1969).

DIFFUSION THERMIQUE DANS UN MILIEU POREUX À PARTIR D'UNE CONDENSATION DE VAPEUR

Résumé—L'effet de transfert thermique dans un milieu poreux provoqué par la condensation a été traité théoriquement. Les équations basées sur le concept de la chaleur spécifique globale ont été établies.

La chaleur spécifique globale est définie comme suit:

$$C_p = C_{ps} + C_{pr},$$

où C_{ps} est la chaleur spécifique du corps et C_{pr} un terme de chaleur spécifique dû à la contribution de la chaleur latente.

C_{pr} est défini par l'équation;

$$C_{pr} = \Delta H\,(\rho_r/\rho_s)\,(\partial k/\partial T).$$

La conductivité thermique effective est définie comme suit:

$$\lambda_e = \lambda_s + \lambda_f \quad \text{où} \quad \lambda_f = C_{pg}\rho_{pg}D.$$

L'effet de condensation dans les milieux poreux et la distribution de température, ont été numériquement traités par des ordinateurs. Les résultats de l'analyse sont donnés dans les Fig. 3–6. Ils sont en très bon accord avec les résultats observés.

DER WÄRMEÜBERGANG BEI DER DIFFUSION KONDENSIERBARER DÄMPFE DURCH PORÖSE MEDIEN

Zusammenfassung—Der Einfluss der Kondensation auf den Wärmetransport in porösen Stoffen wurde theoretisch behandelt.

Die theoretischen Gleichungen wurden auf der Grundlage der gesamten spezifischen Wärmekapazität abgeleitet. Die gesamte spezifische Wärme ist folgendermassen definiert; $C_p = c_{ps} + c_{pr}$, wobei c_{ps} die spezifische Wärmekapazität des Körpers und c_{pr} den Wert der spezifischen Wärmekapazität aufgrund des Beitrags der Verdampfungswärme bedeuten. Der Wert c_{pr} wird ausgedrückt durch die Gleichung $c_{pr} = \Delta H^{*}\rho_r/\rho_s).(\partial K/\partial T)$. Die effektive Wärmeleitfähigkeit wird definiert durch $\lambda_e = \lambda_s + \lambda_f$, wobei $\lambda_f = c_{pg}\rho_{gp}.D$ ist.

Das Ausmass der Kondensation und die Temperaturverteilung in porösen Körpern wurden durch Computer analysiert. Die theoretischen Ergebnisse wurden mit beobachteten Werten verglichen.

Die Ergebnisse der Untersuchung sind in Fig. 3 bis 6 dargestellt. Sie stimmen mit beobachteten Werten einigermassen überein.

ТЕПЛООБМЕН В ПОРИСТЫХ СРЕДАХ, ДИФФУНДИРУЮЩИХ В КОНДЕНСИРУЮЩЕМСЯ ПАРЕ

Аннотация—Теоретически исследуется влияние переноса в пористых средах под влиянием конденсации.

Получены аналитические уравнения на основе понятия суммарной удельной теплоемкости. Суммарная удельная теплоемкость определяется в виде $C_p = c_{ps} + c_{pr}$, где c_{ps} — удельная теплоемкость тела, а c_{pr} — величина удельной теплоемкости, обусловленной вкладом скрытой теплоты.

c_{pr} — выражается уравнением $c_{pr} = \Delta H(\rho_r/\rho_s)(\partial \bar{k}/\partial T)$.

Эффективная теплопроводность определяется в виде $\lambda_e = \lambda_s + \lambda_f$, где $\lambda_f = c_{pg}$.

На электронных машинах проведен численный анализ распределения температуры и степени конденсации в пористом теле. Теоретический расчет сравнивается с имеющимися данными.

Результаты анализа представлены на рис. 3–6. Они хорошо согласуются с экспериментальными данными.